
Mixture of Experts with Uncertainty Voting for Imbalanced Deep Regression Problems

Yuchang Jiang
University of Zurich

Vivien Sainte Fare Garnot
University of Zurich

Konrad Schindler
ETH Zurich

Jan Dirk Wegner
ETH Zurich & University of Zurich

Abstract

Data imbalance is ubiquitous when applying machine learning to real-world problems, particularly regression problems. If training data are imbalanced, the learning is dominated by the densely covered regions of the target distribution, consequently, the learned regressor tends to exhibit poor performance in sparsely covered regions. Beyond standard measures like over-sampling or re-weighting, there are two main directions to handle learning from imbalanced data. For regression, recent work relies on the continuity of the distribution; whereas for classification there has been a trend to employ mixture-of-expert models and let some ensemble members specialize in predictions for the sparser regions. Here, we adapt the mixture-of-experts approach to the regression setting. A main question when using this approach is how to fuse the predictions from multiple experts into one output. Drawing inspiration from recent work on probabilistic deep learning, we propose to base the fusion on the aleatoric uncertainties of individual experts, thus obviating the need for a separate aggregation module. In our method, dubbed MOUV, each expert predicts not only an output value but also its uncertainty, which in turn serves as a statistically motivated criterion to rely on the right experts. We compare our method with existing alternatives on multiple public benchmarks and show that MOUV consistently outperforms the prior art, while at the same time producing better calibrated uncertainty estimates. Our code is available at *link-upon-publication*.

1 Introduction

Data imbalance is the norm, rather than the exception in real-world machine learning applications, and in regression tasks, in particular. Outside the realm of carefully curated research datasets, the distribution of the target values is typically non-uniform. Some parts of the distribution are covered by training examples much more densely than others, and as a result, machine learning models tend to be biased towards those well-represented regions and perform poorly in under-represented ones He and Garcia [2009]. What is more, these sparse regions of the distribution are often important. In several applications, the prediction results matter specifically for rare, unusual conditions like extreme wind speeds in meteorology Maskey et al. [2020], or particularly high biomass in vegetation mapping Lang et al. [2022]. Therefore, addressing the imbalance problem is an active area of machine learning research.

Traditional attempts to mitigate the impact of imbalance rely either on over-sampling rare data samples or on re-weighting the loss function to increase the cost of prediction errors at rare samples He and Garcia [2009]. More recently, several authors have revisited the issue in the context of deep learning, typically through variants of the *mixture of experts* framework. An ensemble of "expert" models is trained in such a way that they can each attend to a different part of the distribution. Then

their predictions are aggregated to obtain the final inference. The challenge in such methods consists in ensuring complementarity between the different experts and designing an aggregation method that synthesizes the predictions of individual ensemble members according to their relevance. A naive solution is to use the ensemble average, but this risks giving too much weight to predictions that are irrelevant to the specific data point. More elaborate solutions tune the aggregation weights in an unsupervised fashion [Zhang et al., 2021]. Once optimized, these weights are still fixed and subject to the same limitation. It has also been proposed to use dynamic weights obtained from a *sample-level* voting module that is trained with an independent objective [Wang et al., 2020]. All works mentioned so far focus on classification problems. *Imbalanced regression*, on the other hand, has been studied a lot less and has only recently started to gain attention, especially since the publication of a suitable benchmark [Yang et al., 2021]. The prevalent idea so far has been to exploit the continuity of regression functions, either by smoothing the features and labels [Yang et al., 2021] or by regularizers that encourage similar latent features at similar (continuous) labels [Gong et al., 2022]. On the contrary, the mixture-of-experts idea has barely been explored in the context of imbalanced regression, despite the fact that model ensembles are common for deep regression [Lang et al., 2022, Yeo et al., 2021, Becker et al., 2023].

Here, we introduce a mixture of experts model with uncertainty voting (MOUV) for deep imbalanced regression. We adopt the expert ensemble framework for regression and propose a principled and straightforward way to dynamically aggregate the predictions. Rather than adding an empirically designed or learned voting module, we leverage the fact that uncertainty estimation techniques for deep regression [Kendall and Gal, 2017] inherently compute statistically meaningful weighting coefficients. Specifically, we use the estimated aleatoric uncertainties of individual experts to combine their predictions. To achieve this with a low computational overhead, we follow recent literature [Zhou et al., 2020] and construct a light ensemble, consisting of a shared encoder backbone and separate decoding branches for different experts. We experimentally evaluate our approach against other methods for deep imbalanced regression on a diverse set of tasks, including age regression, meteorological prediction, and text similarity prediction. We show that MOUV sets a new state-of-the-art performance on three out of four tasks and performs competitively on the last. Importantly, while MOUV improves overall performance, the gains are most significant for rare output values that are under-represented in the training data. In a large part, these gains can be attributed to the uncertainty-based aggregation. As an additional benefit, the uncertainties predicted by MOUV are better calibrated and, therefore, more informative for downstream tasks that rely on the regression output. Following this approach, we integrate uncertainty estimates from experts who specialize in different data distributions to mitigate the impact of imbalanced data on regression.

To summarize, our contributions are:

- We introduce MOUV, a novel, efficient end-to-end method for imbalanced regression.
- We show empirically on four different datasets that MOUV advances the state of the art in terms of both the regression errors and the associated uncertainty estimates.
- To the best of our knowledge, MOUV is the first deep imbalanced regression method that combines the mixture-of-experts scheme with ideas from probabilistic deep learning.

2 Related Work

Imbalanced Regression As imbalanced regression receives less attention than imbalanced classification, early works usually use methods originally proposed for imbalanced classification. For example, the Synthetic Minority Oversampling Technique (SMOTE) introduced in Chawla et al. [2002] can create synthetic samples to relieve the imbalance in classification, which is also applied in regression problems Branco et al. [2017]. Similarly, Lang et al. [2022] follows the class-balanced loss idea to add frequency-based weights to the loss function, so the model pays more attention to minority samples. More recently, Yang et al. [2021] introduces a public benchmark for imbalanced regression and investigates the continuity nature of regression problems with label and feature smoothing techniques. This public benchmark has encouraged more work focusing on the imbalanced regression. Then Gong et al. [2022] proposes a ranking-based regularization method to utilize the continuity property of the regression targets and enhance representation learning in the imbalanced regression.

Imbalanced Classification Most works studying imbalanced dataset focus on classification tasks. Early works include re-weighting Cui et al. [2019], re-sampling, Chawla et al. [2002] and data augmentation Zhang et al. [2017]. A recent direction in imbalanced classification is the mixture-of-expert idea. Wang et al. [2020] proposes a two-stage method: in the first stage, they optimize three experts as three branches and use Kullback–Leibler divergence in the loss function to encourage expert diversity; in the second stage, they aggregate experts by training binary classifiers as dynamic expert assignment modules. Zhang et al. [2021] enforces different distribution for each expert explicitly to ensure the diversity of experts and utilizes a self-supervised training method at the test stage to combine experts for the final output. Although Zhang et al. [2021] requires no additional training for expert aggregation, the learnt weights are fixed at the *dataset-level* instead of *sample-level*. Our work adapts the mixture-of-expert idea to regression task and we propose a new uncertainty-based expert aggregation mechanism, which requires no additional training and combines experts based on per-sample weights.

Application of Uncertainty Estimation probabilistic deep learning methods like Kendall and Gal [2017] estimate both the mean target value and the uncertainty, which helps the model interpretation. Recent works further use uncertainty to achieve stronger predictions instead of solely producing uncertainty as a nice-to-have output. Yeo et al. [2021] utilizes a ensemble of probabilistic deep learning models to increase robustness to domain shifts. Each member of the ensemble is uniquely perturbed during training, and the aggregated ensemble prediction via the corresponding uncertainty achieves a more robust prediction against image corruption. Similarly, Becker et al. [2023] combines the predictions based on uncertainty to generate the country-wide map of forest structure variables, which is more robust to clouds. Here we also use estimated uncertainty to aggregate the knowledge of experts but our method is different from the previous methods in two aspects. First, we use multiple branches trained with different losses instead of a simple ensemble of models with different initializations, which is more computationally efficient. The second difference is the source of diversity among experts. Instead of relying on the randomness or the specified middle domain, we encourage different data distributions for each expert to achieve diverse predictions.

3 Method

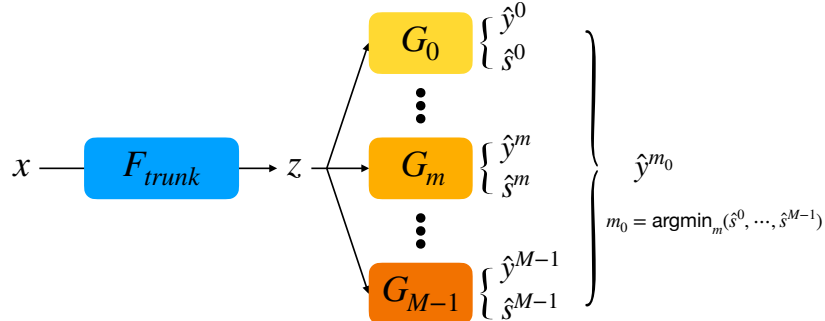


Figure 1: **Overview of MOUV.** A shared backbone encodes the input x into a representation z . A mixture of M different experts use this shared representation to make their predictions. Each expert predicts a regression value \hat{y} as well as the uncertainty \hat{s} of that prediction. At inference time, we use the prediction of the most certain expert m_0 .

Figure 1 shows a schematic overview of MOUV, the following paragraphs describe its components. MOUV consists of joint training of M different regression experts. Each expert predicts a sample-dependent aleatoric uncertainty, and that uncertainty is used to combine the predictions.

We consider a generic univariate regression dataset $\mathcal{D} = \{(x_n, y_n), n \in \llbracket 1, N \rrbracket\}$ of size N , with x_n the input tensors, and y_n the corresponding scalar target values. We define B equally spaced bins across the target range and approximate the frequency distribution of the data by counting the number of data points per bin, $\mathbf{f} = (f_1, \dots, f_B)$.

Multi-headed architecture Instead of training M independent models, we follow recent literature Zhou et al. [2020] and design a multi-headed architecture with a shared backbone encoder and M regression heads that act as different experts. This design has the advantage that it is computationally lightweight and lets all experts rely on a common representation. The shared backbone encoder F_{trunk} can be selected according to the task at hand and maps each input point x_n to an embedding z_n . The latter is processed by M different regression heads G_m that each output their individual expert prediction.

Aleatoric uncertainty prediction Each expert m makes two predictions: the target value \hat{y}_n^m and its associated aleatoric uncertainty \hat{s}_n^m . Following Yeo et al. [2021], we train these predictions by minimizing the negative log-likelihood of the Laplace distribution:

$$\hat{y}_n^m, \hat{s}_n^m = G_m(z_n), \quad (1)$$

$$\mathcal{L}_{NLL}^m = \frac{1}{N} \sum_{n=1}^N w_n^m \exp(-\hat{s}_n^m) \|y_n - \hat{y}_n^m\|_1 + \hat{s}_n^m. \quad (2)$$

For numeric stability, we optimize \hat{s}_n , the logarithm of the scale parameter in the Laplace distribution.

Joint training of diverse experts Each expert m is trained with a different weighting of the samples w_n^m , so as to achieve diversity and to make experts focus on different parts of the target distribution. The weights for expert m are defined as:

$$w_n^m = \left(\frac{1}{f_{b(n)}} \right)^{p_m}, \quad (3) \quad \text{with } p_m = \frac{m}{M-1}, m \in \{0, \dots, M-1\}, \quad (4)$$

with $b(n)$ the bin in which sample n falls. Parameter p_m controls how strongly an expert concentrates on samples from sparse regions of the input distribution, with larger p corresponding to stronger rebalancing: when $p = 0$, the expert treats each sample equally; when $p = 1$, the expert employs inverse-frequency weighting and fully compensates density variations in the input. Different settings of p are complementary: unweighted standard regression learns the correct frequency prior and gives all data points the same influence on the latent representation; whereas inverse frequency weighting ensures that the model is not dominated by the dense regions of the distribution and fails to learn about the sparse ones. Intermediate versions between those extremes, like the popular inverse-squareroot weighting Lang et al. [2022], attempt to find a compromise. Together, the ensemble of experts strikes a balance by offering solutions according to several different weighting schemes and picking the least uncertain one on a case-by-case basis.

Dynamic learning For representation learning, it is arguably more correct to assign samples equal weight. It is not obvious why the feature extractor that transforms raw data into a latent representation should to a large degree depend on the properties of rare, potentially not overly representative samples. Inspired by Zhou et al. [2020], we employ a dynamic learning strategy that initially focuses on the latent encoding and gradually phases in the remaining experts that have unequal weighting schemes:

$$\mathcal{L} = \alpha \mathcal{L}_{NLL}^0 + (1 - \alpha) \sum_{m=1}^{M-1} \mathcal{L}_{NLL}^m, \quad (5) \quad \alpha = 1 - \left(\frac{T}{T_{max}} \right)^2, \quad (6)$$

where T is the current epoch number, and T_{max} is the maximum epoch number. \mathcal{L}_{NLL}^0 is the loss for the expert with $m = 0$, which treats all samples equally. α balances representation learning against mitigating the data imbalance.

Uncertainty-based expert aggregation During inference time, the predictions from multiple experts are combined based on the estimated uncertainty. One natural solution would be to weight the predictions using the inverse uncertainties. However, we obtain better experimental performance with selecting the output with the lowest predicted uncertainty:

$$\hat{y}_n = \hat{y}_n^{m_0}, \quad \hat{s}_n = \hat{s}_n^{m_0} \quad (7)$$

$$\text{with } m_0 = \operatorname{argmin}_m (\hat{s}_n^1, \dots, \hat{s}_n^M). \quad (8)$$

4 Experiments

4.1 Datasets

We evaluate our method on the four public regression datasets: **AgeDB** Moschoglou et al. [2017], Yang et al. [2021] is an age estimation dataset and it consists of 12208 training images, 2140 validation images, and 2140 test images. **IMDB-WIKI** Rothe et al. [2018], Yang et al. [2021] is an age dataset consisting of 191509 training samples, 11022 validation samples, and 11022 test samples. **Wind** Maskey et al. [2020] is a wind speed estimation dataset consisting of satellite images. It contains 54735 images for training, 14534 images for validation, and 44089 images for testing. The wind speed ranges from 0 to 185 *kn*. **STS-B** Cer et al. [2017], Wang et al. [2018], Yang et al. [2021] is a semantic textual similarity benchmark, consisting of sentence pairs with a similarity score ranging from 0 to 5. It contains 5249 training samples, 1000 validation samples, and 1000 test samples. The four datasets have diverse imbalance factors, ranging from 353 to 5400.

Figure 2 shows an overview of the distribution of all datasets. Note the irregular distribution of the Wind dataset, potentially caused by rounding artifacts, but already present in the dataset’s release article (see Fig. 2 of Maskey et al. [2020]). **STS-B** also displays an irregular distribution, likely linked to the similarity scores obtained by averaging values from multiple subjective human annotations. We find experimentally that estimating frequencies with kernel density estimation (KDE) leads to more robust performance than with simple histograms for such irregular distributions. We thus replace $f_{b(n)}$ in Eq. 3 with the sample-level estimated density for these two datasets:

$$\hat{f}(x) = \frac{1}{Nh} \sum_{n=1}^N K\left(\frac{x - x_n}{h}\right), \quad (9)$$

with K the Gaussian kernel, and h set to 1 for **Wind**, and 0.5 for **STS-B**. Methods using KDE for frequency estimation are denoted by κ in the rest of the paper.

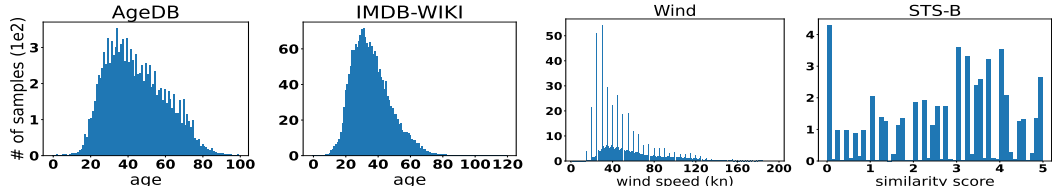


Figure 2: **Dataset overview.** Distribution of the training set of the four datasets. We consider very different tasks ranging from age regression, to text similarity prediction, and wind speed estimation.

4.2 Experimental Setup

Competing methods We benchmark our approach against a vanilla backbone and a comprehensive set of recent state-of-the-art methods:

- **Vanilla** is the baseline model without specified techniques for imbalanced regression
- **RRT** is a two-stage training method: after training the model normally in the first stage, the regressor is re-trained with a rebalanced loss function.
- **SQINV/INV** uses inverse frequency weighting (for **STS-B**) and inverse-squareroot frequency weighting (for the remaining datasets) in the loss function, following Yang et al. [2021].
- **LDS+FDS** are the label and feature smoothing functions introduced by Yang et al. [2021]
- **RankSim** is a regularization technique proposed by Gong et al. [2022], which encourages data points that have more similar target values to also lie closer to each other in feature space, by aligning the corresponding rank orders

The baselines methods are to some degree complementary and can be combined. We therefore also test combinations of them as, e.g., LDS+FDS is a reweighting of features and loss terms, and RankSim is an additional regularizer that can be combined with different loss functions. For **AgeDB**, **IMDB-WIKI**, and **STS-B** datasets, the performance metrics for the baselines are taken from Yang et al. [2021], Gong et al. [2022]. The **Wind** dataset is not included in that benchmark, so we run the baselines, using the official, public implementations of Yang et al. [2021], Gong et al. [2022].

Metrics Following Yang et al. [2021], we report the Mean Absolute Error (MAE) to evaluate regression performance on the **AgeDB**, **IMDB-WIKI**, and **Wind** datasets. Some work also reports Geometric Mean (GM), but in practice that metric strongly correlates with the MAE. For completeness we report it in the supplementary material. To be comparable, we follow Cer et al. [2017] for **STS-B** and report the Pearson correlation coefficient, expressed as a percentage ($P\%$). We also report the Mean Squared Error (MSE) of **STS-B** in the supplementary material. We report these metrics on the complete test set (All), as well as separately for different data density regimes. To that end the test data are binned into a frequency distribution. Bins with >100 samples form the many-shot regime (denotes *many* in the tables), bins with 20 to 100 samples form the medium-shot (*med.*) regime, and bins with <20 samples are the few-shot (*few*) regime Yang et al. [2021]. Similar to other studies, we use bins of size 1 on **AgeDB**, **IMDB-WIKI**, and **Wind**, and of size 0.1 on **STS-B**. We report the Uncertainty Calibration Error (UCE) to evaluate the quality of the predicted uncertainties.

Implementation details All codes to conduct the experiments is implemented in Pytorch Paszke et al. [2019]. We use ResNet-50 as backbone for **AgeDB** and **IMDB-WIKI**, and ResNet-18 for **Wind**. For **STS-B**, we use BiLSTM+GloVe as the baseline, following Wang et al. [2018]. The number of experts in MOUV (M) is tuned by training different instances and selecting the best one based on validation set performance. This gives $M = 2$ for **AgeDB** and **Wind**, and, $M = 3$ for **IMDB-WIKI** and **STS-B**. For further details about model training, see the supplementary material.

4.3 Imbalanced Regression Experiment

Comparison to state-of-the-art We report the numerical results of our experiments in Table 1. In terms of overall performance, MOUV outperforms all existing approaches on **AgeDB**, **IMDB-WIKI**, and **Wind** and is a close second on the **STS-B** dataset. On **AgeDB**, **IMDB-WIKI**, and **Wind**, our work also achieves the best performance on the *medium-shot* and *few-shot* regions of the distribution. The gain in few-shot performance compared to the Vanilla model ranges from 43% on **AgeDB** to 20% on **IMDB-WIKI**. The margin w.r.t. the closest competitor ranges from 21% on **AgeDB** to 3% on **Wind**. At the same time, MOUV still reaches the second-best performance in data-rich region (*many*), highlighting that it indeed leverages the predictions of different experts to respond to imbalanced datasets with marked density variations. On the **STS-B** dataset, MOUV achieves the second-highest Pearson correlation overall, as well as in the *medium-density* regime, and the highest one for the *many-shot* regime. On the contrary, in the *few-shot* setting it does not shine, although it still outperforms not only the Vanilla model, but also standard baselines like RRT, LDS+FDS, and INV. For this particular dataset, RankSim clearly appears to be a more suitable strategy. We speculate that this may be due to the irregular distribution and the subjectively defined, non-metric target signal, for which it is challenging to obtain well-calibrated uncertainties. It appears that an approach based on pairwise feature similarity like RankSim, rather than metric uncertainty, is better suited for such data.

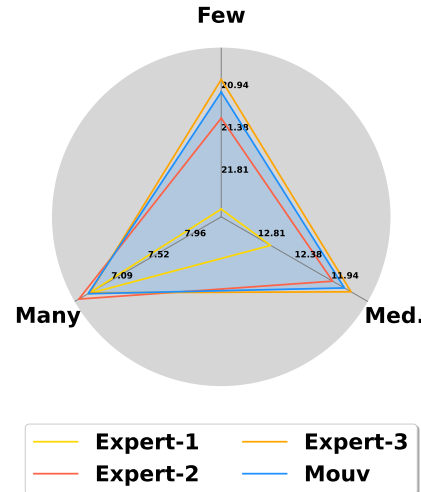


Figure 3: Per-expert and aggregated MAE on **IMDB-WIKI**. The uncertainty-based aggregation of MOUV nearly matches the performance of the best available expert on each subset of the test data.

Table 1: **Main experiment.** We report the regression performance (MAE \downarrow for AgeDB, IMDB-WIKI, Wind datasets, Pearson correlation (%) \uparrow for STS-B). For each column, the best results are in **bold** and the second best results are underlined.

	AgeDB \downarrow				IMDB-WIKI \downarrow			
	All	Many	Med.	Few	All	Many	Med.	Few
		Many	Med.	Few		Many	Med.	Few
Vanilla	7.77	6.62	9.55	13.67	8.06	7.23	15.12	26.33
+RankSim	7.13	<u>6.51</u>	8.17	10.12	7.72	6.93	14.48	25.38
RRT	7.74	6.98	8.79	11.99	7.81	7.07	14.06	25.13
+LDS,FDS	7.66	6.99	8.60	11.32	7.65	7.06	12.41	23.51
+RankSim	7.11	6.53	8.00	10.04	7.55	6.83	13.47	24.72
+LDS,FDS+RankSim	7.13	6.54	8.07	10.12	7.37	6.80	<u>11.80</u>	23.11
SQINV	7.81	7.16	8.80	11.20	7.87	7.24	12.44	22.76
+LDS,FDS	7.55	7.01	8.24	10.79	7.78	7.20	12.61	22.19
+RankSim	<u>6.91</u>	6.34	7.79	<u>9.89</u>	7.42	6.84	12.12	22.13
+LDS,FDS+RankSim	7.03	6.54	<u>7.68</u>	9.92	7.69	7.13	12.30	<u>21.43</u>
MOUV	6.82	6.55	7.37	7.80	7.36	<u>6.81</u>	11.78	20.96
Wind \downarrow								
	All	Many	Med.	Few	All	Many	Med.	Few
Vanilla	7.48	7.38	13.10	21.42	74.2	72.0	62.7	75.2
+RankSim	<u>7.43</u>	<u>7.33</u>	12.49	20.50	76.8	71.0	72.9	85.2
RRT	7.51	7.39	13.67	22.79	74.5	72.4	62.3	75.4
+LDS,FDS	7.52	7.40	13.64	22.35	76.0	73.8	65.2	76.7
+RankSim	7.44	7.34	12.73	21.03	77.1	72.2	68.3	86.1
+LDS,FDS+RankSim	7.45	7.35	12.75	20.93	76.6	71.7	68.0	<u>85.5</u>
SQINV/INV	7.90	7.82	<u>11.97</u>	20.26	72.8	70.3	62.5	73.2
+LDS,FDS	7.75	7.68	<u>11.98</u>	<u>15.87</u>	76.0	<u>74.0</u>	65.2	76.6
+RankSim	7.79	7.71	12.22	20.07	69.9	65.2	60.1	76.0
+LDS,FDS+RankSim	7.71	7.63	12.16	16.70	75.8	70.6	69.0	82.7
MOUV κ	7.30	7.23	11.09	15.43	<u>77.0</u>	74.3	<u>70.0</u>	77.9

In summary, MOUV sets a new state of the art for three of the four datasets, while on **STS-B** it is close second overall, but struggles in the *few-shot* regime. MOUV is very flexible and can be readily adapted to different tasks and instantiated with different encoder and decoder architectures. It comes at a marginal computational cost. For instance, when using ResNet50 as backbone, each expert only increases the parameter count by 0.01%.

Successful expert aggregation As visually illustrated in Figure 3 and numerically supported in Sec. 4.4, the uncertainty component of MOUV is able to dynamically select the expert that makes the best prediction, in the majority of cases: the prediction quality of the ensemble comes close to the one of an oracle that always picks the right expert, across all data regimes.

Uncertainty prediction To assess the reliability of the predicted uncertainty itself, we calculate the uncertainty calibration metric in Table 2. Unsurprisingly, we observe the same pattern as for the actual regression targets: uncertainty is more difficult to estimate in the few-shot regime, i.e., in areas of low sample density. MOUV outperforms the vanilla network, trained with negative log-likelihood (NLL) loss, and the largest gains occur in the few-shot regime. e.g., the uncertainty calibration error (UCE) for samples from few-shot regions drops by 41% on **AgeDB** and by 37% on **Wind**.

Table 2: **Uncertainty calibration.** UCE of MOUV vs. Negative log-likelihood (NLL).

	AgeDB ↓				IMDB-WIKI ↓				Wind ↓				STS-B ↓			
	All	Many	Med.	Few	All	Many	Med.	Few	All	Many	Med.	Few	All	Many	Med.	Few
NLL	1.76	1.05	2.66	6.01	2.36	1.83	7.37	17.71	6.68	6.59	11.52	20.95	0.68	0.65	0.77	0.71
MOUV	1.08	0.72	2.69	3.54	1.94	1.37	6.57	15.74	6.49	6.44	9.45	13.20	0.64	0.62	0.71	0.69

4.4 Ablation Study

We investigate the contribution of different design choices in our method by training the following variants on the same benchmark data:

- **NLL**: The Vanilla architecture, but trained with negative log likelihood loss (NLL), instead of a standard L1 or L2 loss.
- **2-branch, 3-branch**: The multi-head setup of our model without uncertainty estimation, corresponding to a naive model ensemble. We train both a two-branch (2-branch) and a three-branch (3-branch) version.
- **avg-vote**: This approach only differs from MOUV in that it combines the expert predictions by averaging, rather than based on the estimated uncertainty.
- **inv σ -vote**: Here, instead of selecting the lowest-uncertainty prediction in MOUV, we compute the weighted average of all experts’ predictions based on invert uncertainty.
- **oracle-vote**: As an upper bound for the performance of MOUV, we also report the performance it would achieve if it had access to an oracle that selects the best expert for each data point (instead of using the predicted uncertainty).

Probabilistic training Running a single-head regression network, but replacing the standard regression loss (Vanilla) with the NLL loss already leads to an increase in overall performance across all four datasets. On three of the four datasets, performance in the *few-shot* regime also improves by

Table 3: **Ablation study.** We report the regression performance (MAE \downarrow for AgeDB, IMDB-WIKI, Wind datasets, Pearson correlation (%) \uparrow for STS-B) for simplified baseline variants of MOUV.

	AgeDB ↓				IMDB-WIKI ↓			
	All	Many	Med.	Few	All	Many	Med.	Few
Vanilla	7.77	6.62	9.55	13.67	8.06	7.23	15.12	26.33
NLL	7.05	6.24	8.11	11.80	7.57	6.81	13.95	25.67
2-branch	7.68	7.03	8.80	10.66	7.86	7.27	12.69	22.70
3-branch	7.80	7.19	8.93	10.44	7.61	7.03	12.21	22.46
avg-vote	6.81	6.36	7.61	8.89	7.34	6.77	12.06	21.30
inv σ -vote	6.80	6.38	7.58	8.66	7.34	6.77	12.01	21.23
oracle-vote	6.13	5.76	6.85	7.59	6.86	6.31	11.29	20.59
MOUV	6.82	6.55	7.37	7.80	7.36	6.81	11.78	20.96
	Wind ↓				STS-B ↑			
	All	Many	Med.	Few	All	Many	Med.	Few
Vanilla	7.48	7.38	13.10	21.42	74.2	72.0	62.7	75.2
NLL	7.36	7.26	12.74	22.67	76.2	73.5	68.7	76.8
2-branch κ	7.56	7.49	11.15	17.83	76.0	73.4	68.2	74.0
3-branch κ	7.64	7.54	12.76	19.63	75.9	72.5	71.8	74.5
avg-vote κ	7.30	7.23	11.18	15.90	76.9	74.2	70.3	77.8
inv σ -vote κ	7.30	7.22	11.17	15.88	76.9	74.2	70.3	77.8
oracle-vote κ	7.22	7.15	10.91	15.33	77.1	74.4	70.7	77.9
MOUV κ	7.30	7.23	11.09	15.43	77.0	74.3	70.0	77.9

1 – 2pts. In other words, a probabilistic training objective by itself already mitigates the imbalance problem to some degree.

Multi-head structure Also a multi-head architecture with specialized heads generally boosts overall performance, even without the probabilistic loss. The two and three-branch models (2-branch and 3-branch) improve performance primarily in the *few-shot* regions of the distribution, by ≈ 3 pt MAE on **AgeDB**, **IMDB-WIKI**, and **Wind**, and by ≈ 1 pt $P\%$ on **STS-B**. However, these models tend to suffer in high-density regions: *many-shot* performance is lower on three dataset for the 2-branch model and on two datasets for the 3-branch model.

Uncertainty voting In addition to improving the overall performance, the NLL training objective we use in MOUV allows us to select the best prediction based on aleatoric uncertainty. Compared to the 2-branch and 3-branch models, this brings a more significant improvement in the *few-shot* regime, without sacrificing performance in *many-shot* regions. For instance, MOUV reduces the error on **AgeDB**, by 5.87pt in the *few-shot* region, compared to only 1.87pt and 3.23pt reductions with the NLL and 3-branch models, respectively. At the same time, MOUV still outperforms the Vanilla model in the *many-shot* regime. This highlights how uncertainty-based voting helps to select the correct expert at inference time, which also becomes apparent when comparing MOUV against the avg-vote model. While overall performance is similar, uncertainty voting excels in the *few-shot* regions and consistently beats average voting. Average voting only seems beneficial in the *many-shot* regions, where it brings the benefit of a traditional model ensemble. The performance of the invert uncertainty weighting approach (inv σ -vote) also consistently underperforms in the *medium-shot* and *few-shot* regions. This suggests that in data-scarce parts of the distribution, selecting the best expert leads to better performance than ensembling. Lastly, a comparison of MOUV with oracle-voting bound demonstrates that the proposed uncertainty-based expert selection achieves near-perfect decisions in the medium- and low-density regions. While better uncertainty calibration would certainly help to further improve the results, it seems that the per-expert predictions, rather than the mechanism to combine them, are the current bottleneck.

Table 4: **Impact of KDE.** Relative performance variation when switching from histogram-based frequencies to KDE with MOUV. Improvements with KDE are underlined.

	All	Many	Med.	Few
AgeDB \downarrow	+0.21	+0.43	<u>-0.37</u>	<u>-0.24</u>
IMDB-WIKI \downarrow	+0.03	+0.07	<u>-0.37</u>	0
Wind \downarrow	0	+0.01	<u>-0.45</u>	<u>-3.61</u>
STS-B \uparrow	<u>+0.4</u>	<u>+0.6</u>	<u>-0.9</u>	+2.1

Kernel density estimation. As a last ablation we employ KDE instead of histogram binning to estimate the sample density. Table 4 compares the performance of our method with KDE to the one with simple binning, across all datasets. On **AgeDB** and **IMDB-WIKI**, the MAE differences are marginal (< 0.5 pt) while they are more noticeable on datasets with irregular distribution, especially in the *few-shot* regions. In particular, the MAE drops by 3.61pt in *few-shot* regions of the **Wind** dataset when using KDE in MOUV. The result suggests that the more sophisticated approach to density estimation benefits datasets with irregular distributions, while making little difference for datasets with already relatively smooth distributions. We also re-trained the SQINV and RRT methods on **Wind** with KDE, but did not observe any performance improvement.

5 Conclusion

We have proposed MOUV, a simple and effective method for deep imbalanced regression. Our method, which can be understood as an ensemble over variably rebalanced regressors, can be freely combined with different encoder backbones and comes with negligible computational overhead. To our knowledge, it is also the first approach to deep imbalanced regression that combines the mixture-of-experts concept with ideas from probabilistic deep learning and uncertainty estimation. In experiments on four different datasets, MOUV reaches the best overall performance and sets a new state of the art for three of them. Importantly, our method decreases the prediction error particularly

in under-represented, low-density regions, while maintaining excellent performance in high-density regions. By construction, MOUV provides well-calibrated predictive uncertainties along with the target values, which enhance interpretability of the results and aid downstream tasks.

Broader Impact

Our work can have a positive impact across multiple domains and industries. In healthcare, our methodology can enhance the accuracy of predictive models, leading to improved diagnoses and treatment recommendations, especially on rare cases. It also contributes to fairness and bias mitigation in machine learning, by promoting equitable decision-making processes and mitigating the bias of deep learning models towards over-represented parts of the population.

References

Alexander Becker, Stefania Russo, Stefano Puliti, Nico Lang, Konrad Schindler, and Jan Dirk Wegner. Country-wide retrieval of forest structure from optical and SAR satellite imagery with deep ensembles. *ISPRS Journal of Photogrammetry and Remote Sensing*, 195:269–286, 2023.

Paula Branco, Luís Torgo, and Rita P Ribeiro. SMOGN: a pre-processing approach for imbalanced regression. In *International Workshop on Learning with Imbalanced Domains: Theory and Applications*, pages 36–50, 2017.

Daniel Cer, Mona Diab, Eneko Agirre, Inigo Lopez-Gazpio, and Lucia Specia. Semantic textual similarity—multilingual and cross-lingual focused evaluation. In *Proceedings of the 2017 SEMVAL International Workshop on Semantic Evaluation (2017)*. <https://doi.org/10.18653/v1/s17-2001>, 2017.

Nitesh V Chawla, Kevin W Bowyer, Lawrence O Hall, and W Philip Kegelmeyer. Smote: synthetic minority over-sampling technique. *Journal of Artificial Intelligence Research*, 16:321–357, 2002.

Yin Cui, Menglin Jia, Tsung-Yi Lin, Yang Song, and Serge Belongie. Class-balanced loss based on effective number of samples. In *IEEE/CVF Conference on Computer Vision and Pattern Recognition*, pages 9268–9277, 2019.

Yu Gong, Greg Mori, and Frederick Tung. RankSim: Ranking similarity regularization for deep imbalanced regression. *arXiv preprint arXiv:2205.15236*, 2022.

Haibo He and Edwardo A Garcia. Learning from imbalanced data. *IEEE Transactions on knowledge and data engineering*, 2009.

Alex Kendall and Yarin Gal. What uncertainties do we need in bayesian deep learning for computer vision? *Advances in Neural Information Processing Systems*, 30, 2017.

Nico Lang, Walter Jetz, Konrad Schindler, and Jan Dirk Wegner. A high-resolution canopy height model of the Earth. *arXiv preprint arXiv:2204.08322*, 2022.

Manil Maskey, Rahul Ramachandran, Muthukumaran Ramasubramanian, Iksha Gurung, Brian Freitag, Aaron Kaulfus, Drew Bollinger, Daniel J Cecil, and Jeffrey Miller. Deepti: Deep-learning-based tropical cyclone intensity estimation system. *IEEE Journal of Selected Topics in Applied Earth Observations and Remote Sensing*, 13:4271–4281, 2020.

Stylianos Moschoglou, Athanasios Papaioannou, Christos Sagonas, Jiankang Deng, Irene Kotsia, and Stefanos Zafeiriou. AgeDB: the first manually collected, in-the-wild age database. In *IEEE Conference on Computer Vision and Pattern Recognition Workshops*, pages 51–59, 2017.

Adam Paszke, Sam Gross, Francisco Massa, Adam Lerer, James Bradbury, Gregory Chanan, Trevor Killeen, Zeming Lin, Natalia Gimelshein, Luca Antiga, et al. Pytorch: An imperative style, high-performance deep learning library. *Advances in Neural Information Processing Systems*, 32, 2019.

Rasmus Rothe, Radu Timofte, and Luc Van Gool. Deep expectation of real and apparent age from a single image without facial landmarks. *International Journal of Computer Vision*, 126(2-4):144–157, 2018.

Alex Wang, Amanpreet Singh, Julian Michael, Felix Hill, Omer Levy, and Samuel R Bowman. Glue: A multi-task benchmark and analysis platform for natural language understanding. *arXiv preprint arXiv:1804.07461*, 2018.

Xudong Wang, Long Lian, Zhongqi Miao, Ziwei Liu, and Stella X Yu. Long-tailed recognition by routing diverse distribution-aware experts. *arXiv preprint arXiv:2010.01809*, 2020.

Yuzhe Yang, Kaiwen Zha, Yingcong Chen, Hao Wang, and Dina Katabi. Delving into deep imbalanced regression. In *International Conference on Machine Learning*, pages 11842–11851, 2021.

Teresa Yeo, Oğuzhan Fatih Kar, and Amir Zamir. Robustness via cross-domain ensembles. In *IEEE/CVF International Conference on Computer Vision*, pages 12189–12199, 2021.

Hongyi Zhang, Moustapha Cisse, Yann N Dauphin, and David Lopez-Paz. mixup: Beyond empirical risk minimization. *arXiv preprint arXiv:1710.09412*, 2017.

Yifan Zhang, Bryan Hooi, Lanqing Hong, and Jiashi Feng. Self-supervised aggregation of diverse experts for test-agnostic long-tailed recognition. *arXiv preprint arXiv:2107.09249*, 2021.

Boyan Zhou, Quan Cui, Xiu-Shen Wei, and Zhao-Min Chen. BBN: Bilateral-branch network with cumulative learning for long-tailed visual recognition. In *IEEE/CVF Conference on Computer Vision and Pattern Recognition*, pages 9719–9728, 2020.

A Experimental Settings

A.1 Training Details

AgeDB We use a ResNet-50 backbone for all methods and train each model for 90 epochs with a batch size of 64 and Adam optimizer. The initial learning rate is set as 1×10^{-3} and is scheduled to drop by a factor 10 at epochs 60 and 80. For the last output layers of uncertainty estimation, we set a smaller learning rate, 1×10^{-4} for stable training. In the second training stage of RRT, we utilize an initial learning rate of 1×10^{-4} and train the model for a total of 30 epochs. We use L_1 loss for baselines and Laplacian negative log-likelihood loss for our proposed method. For kernel density estimation, we use the Gaussian kernel with bandwidth 2.

IMDB-WIKI We use ResNet-50 for all experiments and train each model for 90 epochs with batch size 256 and Adam optimizer. The initial learning rate is set as 1×10^{-3} and it is divided by 10 at epochs 60 and 80. For last output layers of uncertainty estimation, we set a smaller learning rate, 1×10^{-4} for stable training. During the second training stage of RRT, we set the initial learning rate to 1×10^{-4} and conducted training for a total of 30 epochs. We use L_1 loss for baselines and Laplacian negative log-likelihood loss for our proposed method. For kernel density estimation, we use the Gaussian kernel with bandwidth 2.

Wind We use ResNet-18 for all experiments and train each model 90 epochs with batch size 64 and Adam optimizer. The initial learning rate is set as 1×10^{-3} and it is scheduled to drop by 10 times at epoch 60 and 80. For last output layers of uncertainty estimation, we set a smaller learning rate, 1×10^{-4} for stable training. In the second training stage of RRT, we conducted training for a total of 30 epochs with an initial learning rate of 1×10^{-4} . We use L_1 loss for baselines and Laplacian negative log-likelihood loss for our proposed method. For kernel density estimation, we use the Gaussian kernel with bandwidth 2.

STS-B We use a two-layer BiLSTM as the encoder to learn features and then a final regressor to output final predictions. We train each model 200 epochs with batch size 16 and Adam optimizer. The learning rate is 2.5×10^{-4} . The hyper-parameter settings for RRT remain consistent throughout both the first and second training stages. We use L_2 loss for baselines and Laplacian negative log-likelihood loss for our proposed method. For kernel density estimation, we use the Gaussian kernel with bandwidth 0.5.

A.2 Evaluation Metrics

We provide the details of the evaluation metrics:

- **MAE:** the mean absolute error

$$MAE = \frac{1}{N} \sum_{n=1}^N |y_n - \hat{y}_n| \quad (10)$$

- **GM:** the geometric mean

$$GM = \left(\prod_{n=1}^N |y_n - \hat{y}_n| \right)^{\frac{1}{N}} \quad (11)$$

- **MSE:** the mean squared error

$$MSE = \frac{1}{N} \sum_{n=1}^N (y_n - \hat{y}_n)^2 \quad (12)$$

- **Pearson correlation:** to evaluate performance on the STS-B dataset

$$P\% = \frac{\sum_{n=1}^N (y_n - \bar{y})(\hat{y}_n - \bar{\hat{y}})}{\sqrt{\sum_{n=1}^N (y_n - \bar{y})^2 \sum_{n=1}^N (\hat{y}_n - \bar{\hat{y}})^2}} \times 100 \quad (13)$$

- **UCE:** the Uncertainty Calibration Error is used to evaluate the quality of the predicted uncertainties

$$UCE = \sum_{b=1}^B \frac{N_b}{N} |MAE(b) - \overline{std(b)}| \quad (14)$$

where N is the total number of samples, B is the total number of bins, N_b is the number of samples falling into bin b , $MAE(b)$ is the MAE of samples in bin b , $\overline{std(b)}$ is the mean standard deviation of samples in bin b , and \hat{y} (resp \bar{y}) the mean predicted (resp. target) value on the test set.

B Additional Results

We present additional results on the four datasets in Tables 5-8. Following other work on deep imbalanced regression, we also provide the Geometric Mean (GM) of the different approaches on **AgeDB**, **IMDB-WIKI**, and **Wind**. We also report the MSE performance on **STS-B**. Overall, the ranking of the compared methods is the same according to either metrics. We observe only two differences: on **IMDB-WIKI** GM gives a marginal advantage in the *many-shot* region to our MOUV method against RRT+LDS,FDS,RankSim; on **STS-B** MSE ranking places INV+LDS,FDS in first position in the *many-shot* region.

Table 5: Complete results on **AgeDB**. For each column, the best results are in **bold** and the second best results are underlined.

	MAE \downarrow				GM \downarrow			
	All	Many	Med.	Few	All	Many	Med.	Few
Vanilla	7.77	6.62	9.55	13.67	5.05	4.23	7.01	10.75
+RankSim	7.13	<u>6.51</u>	8.17	10.12	4.48	<u>4.01</u>	5.27	6.79
RRT	7.74	6.98	8.79	11.99	5.00	4.50	5.88	8.63
+LDS,FDS	7.66	6.99	8.60	11.32	4.80	4.42	5.53	6.99
+RankSim	7.11	6.53	8.00	10.04	4.52	4.19	5.05	6.77
+LDS,FDS+RankSim	7.13	6.54	8.07	10.12	4.55	4.18	5.20	6.87
SQINV	7.81	7.16	8.80	11.20	4.99	4.57	5.73	7.77
+LDS,FDS	7.55	7.01	8.24	10.79	4.72	4.36	5.45	6.79
+RankSim	<u>6.91</u>	6.34	7.79	<u>9.89</u>	<u>4.28</u>	3.92	<u>4.88</u>	6.89
+LDS,FDS+RankSim	7.03	6.54	<u>7.68</u>	9.92	<u>4.45</u>	4.07	5.23	<u>6.35</u>
MOUV	6.82	6.55	7.37	7.80	4.23	4.09	4.55	4.74

Table 6: Complete results on **IMDB-WIKI**.

	MAE \downarrow				GM \downarrow			
	All	Many	Med.	Few	All	Many	Med.	Few
Vanilla	8.06	7.23	15.12	26.33	4.57	4.17	10.59	20.46
+RankSim	7.72	6.93	14.48	25.38	4.27	3.90	10.02	17.84
RRT	7.81	7.07	14.06	25.13	4.35	4.03	8.91	16.96
+LDS,FDS	7.65	7.06	12.41	23.51	4.31	4.07	7.17	15.44
+RankSim	7.55	6.83	13.47	24.72	4.17	3.86	8.66	15.54
+LDS,FDS+RankSim	7.37	6.80	<u>11.83</u>	23.11	<u>4.06</u>	<u>3.84</u>	<u>6.33</u>	14.71
SQINV	7.87	7.24	12.44	22.76	4.47	4.22	7.25	15.10
+LDS,FDS	7.78	7.20	12.61	22.19	4.37	4.12	7.39	12.61
+RankSim	7.42	6.84	12.12	22.13	4.10	3.87	6.74	12.78
+LDS,FDS+RankSim	7.69	7.13	12.30	<u>21.43</u>	4.34	4.13	6.72	<u>12.48</u>
MOUV	7.36	<u>6.81</u>	11.78	20.96	4.01	3.83	5.95	11.06

Table 7: Complete results on **Wind**. κ indicates KDE is used to compute the frequencies.

	MAE \downarrow				GM \downarrow			
	All	Many	Med.	Few	All	Many	Med.	Few
Vanilla	7.48	7.38	13.10	21.42	4.48	4.43	8.75	16.92
+RankSim	7.43	<u>7.33</u>	12.49	20.50	<u>4.45</u>	<u>4.40</u>	8.48	15.73
RRT	7.51	7.39	13.67	22.79	4.48	4.43	9.21	18.50
+LDS,FDS	7.52	7.40	13.64	22.35	4.49	4.43	8.96	17.87
+RankSim	7.44	7.34	12.73	21.03	4.48	4.43	8.77	16.24
+LDS,FDS+RankSim	7.45	7.35	12.75	20.93	4.48	4.43	8.75	16.16
SQINV	7.90	7.82	<u>11.97</u>	20.26	4.81	4.77	7.46	16.27
+LDS,FDS	7.75	7.68	11.98	<u>15.87</u>	4.67	4.63	7.60	<u>13.00</u>
+RankSim	7.79	7.71	12.22	20.07	4.74	4.70	8.29	15.31
+LDS,FDS+RankSim	7.71	7.63	12.16	16.70	4.64	4.60	7.90	14.13
MOUV κ	7.30	7.23	11.09	15.43	4.33	4.29	7.41	12.26

Table 8: Complete results on **STS-B**. κ indicates KDE is used to compute the frequencies.

	MSE \downarrow				Pearson cor. \uparrow			
	All	Many	Med.	Few	All	Many	Med.	Few
Vanilla	0.974	0.851	1.520	0.984	74.2	72.0	62.7	75.2
+RankSim	0.873	0.908	0.767	<u>0.705</u>	76.8	71.0	72.9	85.2
RRT	0.964	0.842	1.503	0.978	74.5	72.4	62.3	75.4
+LDS,FDS	0.903	<u>0.806</u>	1.323	0.936	76.0	73.8	65.2	76.7
+RankSim	0.865	0.876	0.867	0.670	77.1	72.2	68.3	86.1
+LDS,FDS+RankSim	0.882	0.892	0.887	<u>0.702</u>	76.6	71.7	68.0	<u>85.5</u>
INV	1.005	0.894	1.482	1.046	72.8	70.3	62.5	73.2
+LDS,FDS	0.907	0.802	1.363	0.942	76.0	<u>74.0</u>	65.2	76.6
+RankSim	1.091	1.056	1.240	1.118	69.9	65.2	60.1	76.0
+LDS,FDS+RankSim	0.903	0.908	0.911	0.804	75.8	70.6	69.0	82.7
MOUV κ	<u>0.866</u>	0.828	1.017	0.912	<u>77.0</u>	74.3	<u>70.0</u>	77.9

C Further Analysis

C.1 Repetition Analysis

We conduct five runs of our method and SQINV+LDS,FDS on the AgeDB and Wind datasets, each with a different initialization, to assess the impact of randomness in our experiments. Figure 4 presents the MAE obtained by MOUV and SQINV+LDS,FDS on **AgeDB** and **Wind** datasets, accompanied by error bars representing the standard deviation across five experiments. In both datasets, we consistently observe that our method achieves smaller mean MAE values across all regions. Specifically, in the **AgeDB** dataset, the error bars of MAE are relatively small. In the **Wind** dataset, the error bars of MAE are larger in both methods, particularly in the few-shot region, suggesting more variability in performance.

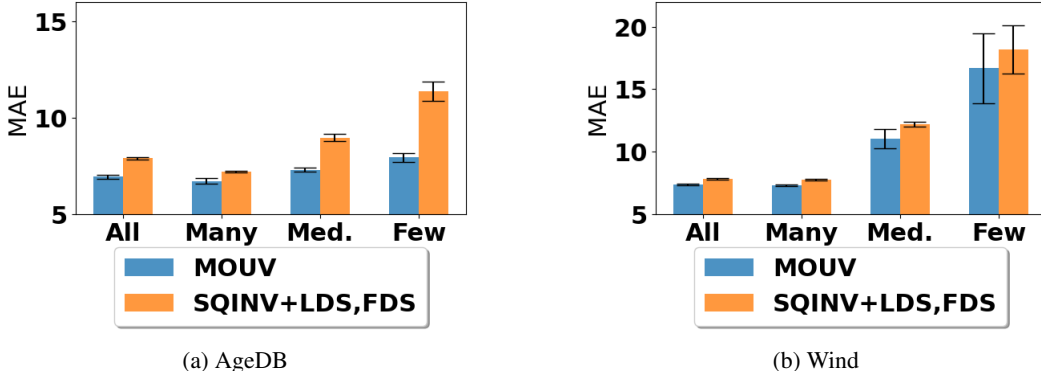


Figure 4: MAE of our methods and SQINV+LDS,FDS on AgeDB and Wind datasets obtained across five models trained with different random initialization.

C.2 Number of branches.

The number of branches is the main hyper-parameter of our method. We present the MAE of models with $M = 1, 2, 3, 4, 5, 6$ in Figure 5. We observe a substantial improvement in MAE within the *few-shot* and *medium-shot* regions when transitioning from a single-expert model to a two-expert model. We note that the performance in the data-scarce parts of the distribution can be further improved by increasing the number of experts, e.g., $M = 4$ in **AgeDB**, which comes, however, at the expense of a slight drop in performance in the many-shot region. In general, our experiments indicate that the configurations with two or three experts achieve best performance across the entire datasets. The optimal number of experts is, of course, problem and dataset-dependent and should be tuned for each application individually.

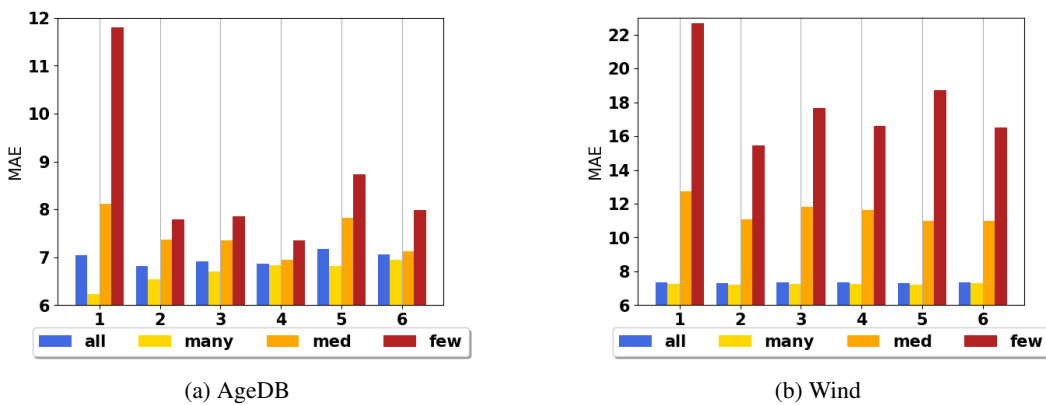


Figure 5: MAE for our methods with different number of experts. In both datasets, the MAE drops sharply when transitioning from a model with a single expert to a model with two experts. Adding more experts brings no major improvements when there are already two or three experts.